Transcription Through Roadblock Systems Reveals A Hybrid Transit Mechanism

Jin Qian,[†] Allison G. Cartee,[†] David Dunlap,[†] Irina Artsimovitch,[‡] and Laura Finzi[*,†]

†*Department of Physics, Emory University, Atlanta, GA*

‡*Department of Microbiology, Ohio State University, Columbus, OH*

E-mail: lfinzi@emory.edu

Abstract

During transcription, RNA polymerases (RNAPs) must transit through roadblocks of various strengths to produce biologically meaningful transcripts. The roadblocking strength of DNA binding proteins varies significantly according to their affinity for DNA. Here we demonstrate that Escherichia coli RNAP can adopt a hybrid mechanism consisting of a passive and an active pathway to effectively transit through two roadblocks of different strengths, the lac repressor protein and EcoRI Q111. The passive pathway, where RNAP waits for the dissociation of the roadblock, is efficient against relatively weak roadblocks. The active mechanism, where RNAP dislodges the roadblock by repetitive cycles of backtracking and recovery, is essential for transit through strong roadblocks. Force direction and transcription factor GreA can bias the choice between the two pathways and modulate the rate of passage through roadblocks. These results further our understanding of how RNAPs transit through roadblocks.

Introduction

DNA is densely covered by proteins for genome organization and function.[1] These DNA-binding proteins play regulatory roles in cellular processes, such as replication and transcription control, recruitment and modulation of processive enzymes, genome condensation.[2–4] However, they must be transiently displaced to allow faithful replication and transcription. DNA-binding proteins vary significantly in their affinity to specific or non-specific DNA sequences, and the affinity may vary with changes in physiological conditions.[5] Therefore, a motor enzyme, such as RNAP, encounters and must displace or wriggle past both low- and high-affinity binding proteins.

Although interference to transcription by roadblocks has been known for decades, its mechanism was determined only in specific cases.[6] In principle, there are two mechanisms by which RNAP could navigate through a protein roadblock. RNAP might passively wait for the spontaneous dissociation of the roadblock or actively dislodge the roadblock protein during the forward translocation step. Previous studies suggest that RNAP likely backtracks at roadblocks and that cooperative convoys of RNAPs, or the presence of anti-backtracking ribosomes on nascent RNA, can promote passage.[7,8] The stability of the backtracked RNAP at the roadblock and backtrack rescue (Gre) factors can also modulate the rate of passage.[9] Yet, these findings were based on run-off transcription assays that do not reveal the dynamics of roadblocked RNAP.

To reveal these dynamics, we monitored real-time transcription of RNAP holoenzyme on DNA templates with either of two roadblock proteins, *lac* repressor or EcoRI Q111, using Magnetic Tweezers (MTs). The experiments were conducted with up to 5 pN forces opposing or assisting RNAP translocation with/without the GreA factor. The roadblock-induced pause times of elongation complexes under different experimental conditions suggest passive or active passages through obstacles with forces and GreA factors determining the choice and efficiency of the alternatives. We propose a model to explain the transit by RNAP through roadblocks.

Results

Forces opposing or assisting RNAP translocation change roadblock-induced pauses

Roadblock-induced transcriptional pauses were measured using digoxigenin-end-labeled DNA templates containing a T7A1 promoter, binding sites for either the lac repressor protein (Os, O1 or O2) or the EcoR1 Q111 protein, and a λT1 terminator (Figure 1a). Biotin-labeled RNAP holoenzyme coupled to streptavidin-coated magnetic beads was introduced in flow chambers containing tethered templates and manipulated in a magnetic tweezer (Figure 1b). Whether force opposed or assisted transcription depended on which end of the template was digoxigenin-labeled and fixed to the glass, while the magnitude was set by the separation between permanent magnets above the flow cell.

Experiments were conducted a forces of 0.2, 0.5, 2.0, and 5.0 pN. Transcription elongation complexes (TECs) paused at *lac* repressor (LacI) binding sites in the presence of the repressor protein but eventually transited through the roadblock (Figure 1c). Different beads exert different forces producing different extensions, so individual records of transcription (tether length versus time) were shifted and scaled to align them. A step-wise fitting algorithm was then applied to produce a dwell-time histogram with distinct peaks at significant pauses and roadblocks. The roadblock-associated pauses were significantly longer than ubiquitous, random, pauses, occured at the protein roadblock binding site, and were identified as the longest pauses within $\pm$ 50 bp of the roadblock binding site . A minor population of traces had no roadblock-associated pauses, likely because of incomplete saturation with roadblock proteins. Pauses shorter than 5 seconds were treated as ubiquitous pauses and were excluded from the analysis. To measure pauses in absence of force, tethered particle motion (TPM) experiments were conducted using similar samples and data processing methods, as described in Materials and Methods.

The RNAP pause lifetimes were distributed exponentially under each and all examined

force conditions, and the characteristic times in each case are plotted in Figure 1d which indicates a significant dependence on the directionality of force (assisting vs. opposing), whereas the magnitude of the force had an negligible effect (Figure 1d). Since RNAP backtracking has been widely reported to be associated with roadblocked transcription, we postulate two explanations for why the average roadblock-induced pause time is shorter under assisting force: assisting force (i) prevents backtracking of TECs, or (ii) helps TECs recover from backtracked states. The results indicate that, unlike sequence-induced backtracking, even a very gentle force of 0.2 pN is sufficient to affect roadblocked TECs.

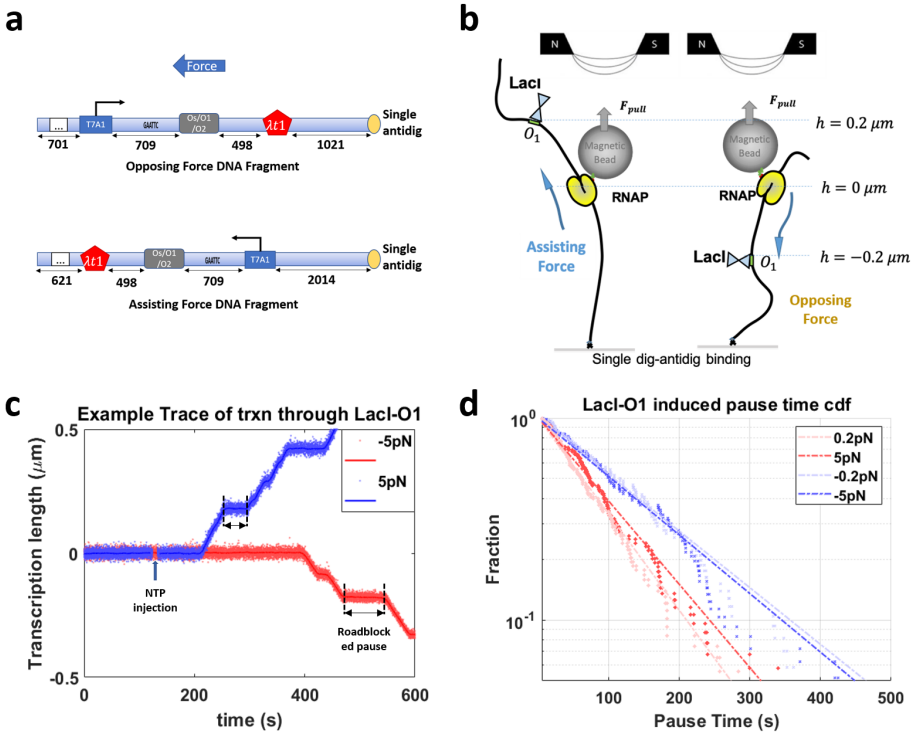

Figure 1: (a) DNA templates for opposing and assisting force experiments . The transcription regions are identical. (b) Experimental setup of the MT experiments. (c) Representative records of transcription through LacI-O1 roadblocks from opposing (red) and assisting (blue) force experiments. Roadblock-induced pauses are bracketed by black dashed lines. (d) Distributions of LacI-O1 induced pause durations under different force conditions and the exponential fits.

GreA shortens the pause time under opposing force by speeding up recovery from the backtracked state

To further investigate how forces affect TECs backtracked at roadblocks, the transcription factor GreA, a factor common to all bacteria that rescues shallowly backtracked TECs, was added to the transcription assays. Addition of GreA had a negligible effect on the pause duration under assisting force but shortened the pauses under opposing force to equal those observed under assisting force (Figure 2b). A simple interpretation is that GreA rescues backtracked RNAPs to increases the rate of passage under opposing force, and that assisting force diminishes backwards translocation of RNAPs into the backtracked state.

For measurements in the presence of the LacI protein, we used DNA templates containing one of three operators, Os, O1 or O2, in order of decreasing affinity. As expected, the average pause time followed the same trend. In addition, similar responses to the direction and magnitude of force and GreA were observed (Figure 2a-c). In all three cases, opposing force was observed to lengthen pauses by $\sim$50 seconds relative to the assisting-force baseline, which in the case of the LacI-O1 and LacI-O2 nucleoprotein complexes, superimposed with baselines in the presence of opposing force with GreA. Indeed, GreA reduced the pause times observed under opposing force with the LacI-O1 and LacI-O2 templates. However, for the LacI-Os template, GreA shortened the pause time under opposing force to less than the assisting-force baseline.

The observed effects of GreA under assisting and opposing force indicate that (i) backtracking rarely occurs under assisting force conditions and (ii) backtracking is responsible for the longer pauses under opposing force conditions. Thus backtracking of TECs did not enhance the passage of RNAP through the LacI-O1 and LacI-O2 roadblocks. In these cases, a passive pathway in which TECs remain transcriptionally active and proceed when roadblocks dissociate appears to be more efficient for overcoming roadblocks. In contrast, to overcome a stronger roadblock like LacI-Os, a combination of backtracking and GreA increased the efficiency of passage.

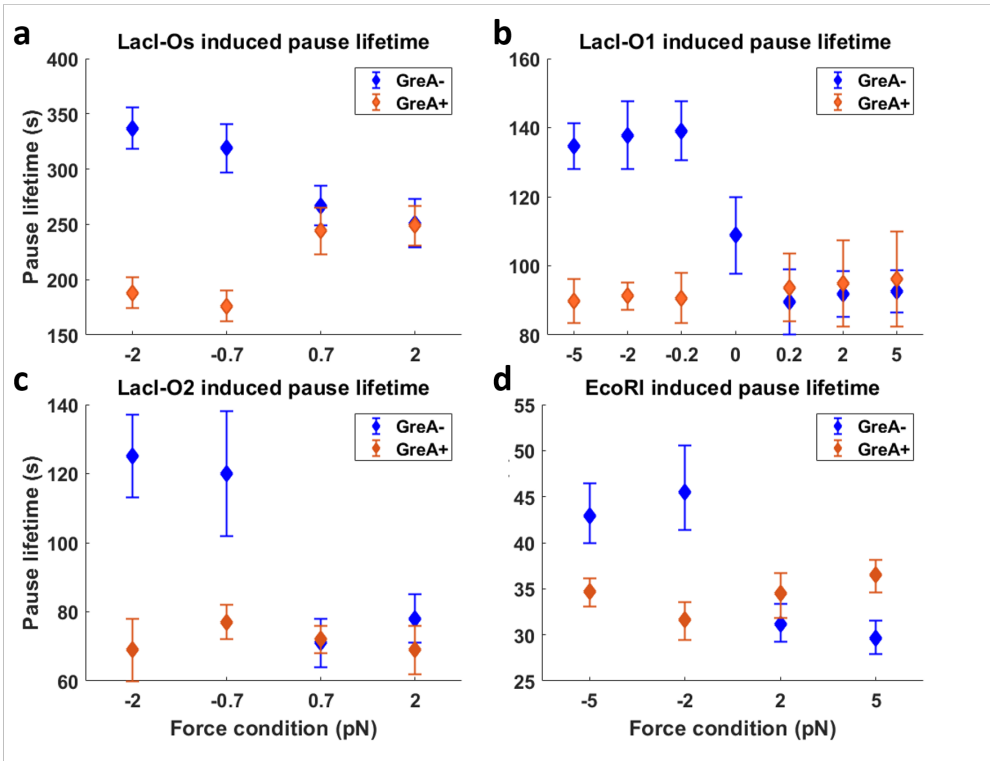

Figure 2: Lifetimes of exponentially distributed pause times under different force and GreA conditions, with (a) LacI-Os, (b) LacI-O1, (c) LacI-O2, and (d) EcoRI Q111 protein roadblocks.

Opposing force and GreA together induce passage through insurmountable roadblocks

Although the passive passage is effective with LacI-O1 and LacI-O2 roadblocks, TECs might traverse roadblocks in other ways, especially those with low dissociation rates. While TECs eventually traversed all LacI-O1 and LacI-O2 roadblocks, the LacI-Os roadblock was insurmountable for a portion of TECs that indefinitely stalled at the roadblock throughout the standard 2-hour recording (Figure 3a). As before the direction of force but not the magnitude altered the ratio of indefinitely stalled TECs, similarly to the trends observed in the pause time distribution. Counter-intuitively, opposing force helped TECs transit through insurmountable roadblocks (FIgure 3b). Addition of GreA led to more successful transits under opposing force but had insignificant effect under assisting force. This observation contradicts with our previous finding that opposing force lengthened pauses at LacI-O1 and LacI-O2 roadblocks. Instead, opposing force enhanced transit of TECs through LacI-Os roadblocks, especially when GreA was present. We speculated that the strength of roadblocks might bias the effects of force and GreA.

To validate this speculation, transcription assays were performed against another strong roadblock, the mutant EcoRI Q111 enzyme. The EcoRI roadblock binds with high affinity to GAATTC sites and successfully blocked nearly 100% of TECs (FIgure 3c) in our standard buffer conditions (20 mM Tris glutamate pH = 8, 50 mM potassium glutamate, 1 0mM magnesium glutamate, 1 mM DTT, 0.2 mg/ml casein). The addition of GreA increased the level of readthrough to 20% only under opposing force conditions (Figure 3c). Curiously, adding GreA to a roadblocked TEC produced passage shortly thereafter (Figure 3a) suggesting that opposing force and GreA might promote transit through insurmountable roadblocks.

With the knowledge that opposing force and GreA together help TEC conquer strong roadblocks, we next investigated the efficiency of passage through the strong roadblocks under stringent conditions (opposing force + GreA). To our surprise, the population that successfully transited through EcoRI roadblocks paused ∼220 seconds (data not shown),

which is similar to the pauses at LacI-Os roadblocks under the same conditions. Opposing force and GreA together may help TECs overcome either type of roadblock. Presumably, LacI-Os is a much weaker roadblock system than the EcoRI roadblock since we observed a significantly higher ratio of successful passage through LacI-Os without GreA. As a result, we speculate that opposing force and GreA may be part of an active pathway for transiting roadblocks of various strengths. The mechanism likely consists of repetitive cycles of backtracking and recovery and functions as a robust mechanism to overcome otherwise insurmountable roadblocks.

Under increased salt concentration (500mM K+), the affinity of EcoRI proteins to the binding site weakens to a level where transcribing polymerases can dislodge a considerable portion of roadblock proteins. Therefore, we collected both the distribution of roadblock induced pause time (Figure 1G) and the ratio of roadblock passage (Figure 2c), as we did with the LacI-Os system. Unlike the long pause lifetime observed in the LacI-Os system, the baseline of assisting-force pause lifetime was only ∼30 seconds. We postulate that this might because high salinity condition modulates the behavior of RNAPs and GreA factors while lowering the binding affinity of EcoRI proteins. The result of roadblock-induced pause time shows similar trend as observed in the relatively weak LacI-O1 and LacI-O2 systems. Opposing force, on one hand, induced longer pause time within the population that successfully transits through roadblock, and the addition of GreA factor brought the opposing force pause time to the same level of assisting-force baseline. On the other hand, opposing force increased overall ratio of TECs passing through the roadblock, and the ratio further increases with the help of GreA.

Discussion

Taken together the observations of the LacI-Os systems and the EcoRI system, an active and a passive pathway of TECs transiting through roadblocks manifest themselves. The passive

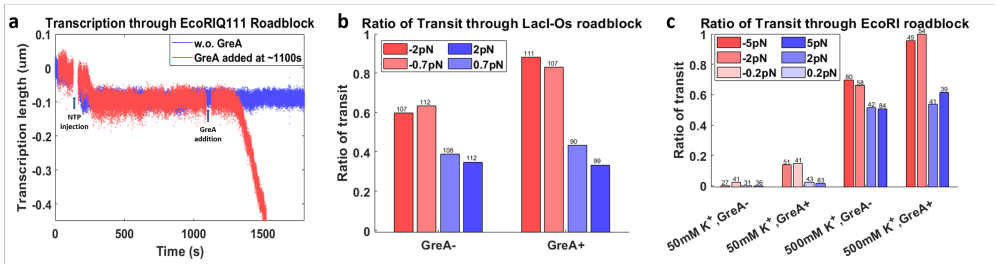

Figure 3: (a) EcoR1 Q111 roadblock indefinitely blocked transcription in absence of GreA factor (blue), and addition of GreA could relieve the blockage (red). (b) Ratio of transit through LacI-Os roadblocks under different force and GreA conditions. (c) Ratio of transit through EcoRI Q111 roadblocks under different salinity, force, and GreA conditions.

pathway occurs when RNAPs dwell at a transcriptionally active state and readily translocate forward as soon as the roadblock disappears. The active pathway occurs when RNAPs tend to actively dislodge the roadblock by repeating the process of backtracking and recovery. We identified that TECs take the passive pathway dominantly under assisting force conditions in the LacI-O1 and LacI-O2 systems and transit through the roadblocks efficiently, whereas in the LacI-Os and EcoRI systems, the active pathway shortens the pause time and induces more successful transits.

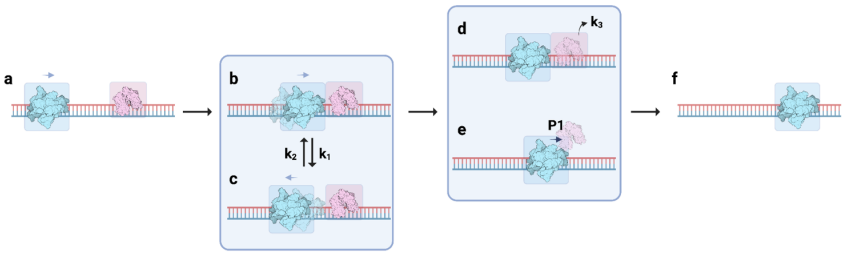

Figure 4: Proposed model of TEC transit through a roadblock. (a) Transcription prior to the encounter of roadblock. (b) TEC encounters the roadblock. (c) TEC backtracks after being roadblocked with a backtracking rate k_1 and recovery rate k_2. (d) Roadblock dissociates from DNA spontaneously with a dissociation rate k_3. (e) An actively transcribing TEC, such as a TEC recovered from backtracked state, has the probability $P1$ of dislodging the roadblock. (f) TEC transits through the roadblock either by actively dislodging the roadblock or after spontaneous dissociation of the roadblock.

Unexpectedly, roadblocked TEC demonstrates such a great sensitivity to external tension

that even 0.2 pN of tension can completely bias its behavior. Tension of such magnitude is prevalent in physiological conditions due to genome anchoring and contacts.[10] Therefore, the passage pathway of roadblocked TECs could be significantly biased by the environment. However, passages of roadblocked TECs also show great insensitivity to the changes in the magnitude of tension, as a same level of roadblock-induced pause time was observed under force magnitude ranging from 0.2 pN to 5pN. This observation is against previous reports that greater opposing force leads to longer backtracked pauses.[11,12] We speculate that the roadblock- induced backtracking process involves a force-sensitive intermediate state followed by a force-insensitive rate-limiting step. Previous study suggests that external forces bias the efficiency of backtracked pauses by modulating the forward transcription rate at backtracking positions, whereas the process of diffusion of backtracked TECs is relatively resistant to external forces.[13,14] Therefore, we speculate that the force-insensitive rate-limiting step is likely the bi-directional diffusion of backtracked TECs, whereas the force-sensitive intermediate might be a state unique to TECs conflicting with roadblock proteins. The difference between roadblock- and sequence-induced backtracks indicates that there might be functional and mechanistic differences between the roadblock and sequence-induced backtracks. The former one helps dislodge strong roadblocks and is easily triggered or dismissed by the change in external tension, while the latter one functions as a universal proofreading mechanism and is more resistant to the change in environment.

Together with the effect of force and GreA factor, we depicted the detailed interconnection between the two pathways in Figure 4. The passive pathway follows the state transition $a \rightarrow b \rightarrow d \rightarrow f$, whereas the active pathway follows $a \rightarrow (b \rightarrow c \rightarrow b)_n \rightarrow e \rightarrow f$ with n cycles of backtracking and recovery. The model consists of three kinetic parameters k_1, k_2 and k_3, which represent the backtrack rate, backtrack recovery rate, and roadblock dissociation rate, respectively. Parameter $P1$ represents the probability of removing roadblock every time an actively transcribing TEC encounters the roadblock. Therefore, the transit rate of the passive pathway is simply $k_{passive} = k_3$, and rate of active pathway is $k_{active} = P_1\ k_1/(1 + k_1/k_2)$.

The overall transit rate is

$$k = \max(k_3, P_1\ k_1/(1 + k_1/k_2)).$$

Our data suggest that under assisting force, backtrack is strictly inhibited and TEC transit occurs after spontaneous dissociation of roadblocks. Thus k_1 is approximately 0 under assisting force, and k_3 can be estimated by the pause lifetime under assisting force. Backtrack recovery rate k_2 should significantly increase in presence of GreA factor. The P_1 of different roadblocks should be scaled with their dissociation rates k_3. All the parameters should be independent of magnitude of force due to the observed magnitude insensitivity in our data. Then the overall transit rate can be simplified to $k = k_3$ under assisting force, and $k = \max(k_3, P_1 \cdot k_1)$ under opposing force with GreA. Therefore, for relatively weak roadblocks where $k_3 > P_1 \cdot k_1$, such as LacI-O1 and LacI-O2, similar pause times were observed under assisting force and opposing force with GreA, whereas for strong roadblocks, opposing force with GreA leads to shorter pause times.

Unfortunately, we cannot directly measure the values of k_1 or P_1 since the two are complementary parts in determining the pause time in the active pathway. However, we observed the active pathway induced similar pause time $\sim$ 200 seconds on two roadblocks LacI-Os and EcoRI of very different strength, indicating that P_1 must change less drastically than the strength of roadblocks. Therefore, $k_1 \cdot P_1$ can give a reasonable rate of transition of most roadblocks in real world. Moreover, the results suggest that the active pathway starts to play important role on roadblock-induced pauses longer than $\sim$ 150 seconds.

In this work, we revealed a hybrid mechanism of TEC transit through roadblocks dependent on their relative strengths. By measuring the dynamics of paused TECs in front of roadblocks, we proposed a two-pathway model and answered the questions about how TECs could transit efficiently through roadblocks of variant strengths. Roadblock strength would bias the selection between the two pathways by modulating their efficiency. Also,

we have found that very low force can completely bias the transit through two types of roadblocks, and we proposed that the roadblock-induced backtracks of TEC may mechanistically differ from the widely studied sequence-induced backtracks. Elucidating the origin of mechanistically different backtracks remains an important subject for future biochemical studies.

Methods and Materials

Preparation of RNAPs and Roadblock Proteins

The β' sub-unit single biotinylated *E. coli* RNAP holoenzymes were reconstituted from the core enzyme variants and σ^{70} initiation factor were expressed as previously described.[15]

Gre factors were purified from plasmids constructed in the Artsimovitch lab as described, analyzed by SDS gel electrophoresis, and tested for RNA cleavage activity. These purified proteins have been crystallized and used in functional and single molecule studies by many groups.[16]

The EcoRI Q111 cleavage-deficient variant has been used extensively for RNA polymerase roadblocking. This protein is expressed in *E. coli* BL21 from a plasmid constructed in the Artsimovitch lab and purified as described.[17] Following purification, the protein was analyzed by SDS gel electrophoresis and tested for DNA binding and transcriptional arrest activities.

Lac repressor protein (LacI) was provided by Kathleen Matthews (Rice University).

Transcription Templates for Magnetic Tweezers Assays

All DNA fragments for MT experiments were PCR amplicons with plasmids pDM_E1_400, pDM_N1_400, pZV_NI_400 or pDM_N2_400 and Q5 Hot Start High-Fidelity 2X PCR Master Mix (New England Biolabs) with single-digoxigenin labeled primers. The transcription region is structured as Promoter-709 bp-Lac operator-498 bp-Terminator with an EcoRI binding sequence GAATTC between promoter and operator sites, as illustrated in Figure

1a. For the opposing force experiments, primers Dig-A/JBOID01-400/5096 and S/JBOID01-400/2086 were used to generate 3k bp DNA fragments with 1021 bp between the chamber surface anchor point and the transcription start site. For the assisting force experiments, primers Dig-S/YY-400-103 and A/PUC18-nuB104/2043 were used to generate 4k bp DNA fragments with 2014 bp between the anchor point and transcription start site. The longer separation in the assisting force DNA fragment reduces adhesion of DNA-attached magnetic beads to the chamber surface at the beginning of transcription. The fragments produced by single-digoxigenin labeled primers generated torsionally unconstrained tethers for the following transcription assays.

Microchamber Preparation and Assembly of Transcription Tethers

Microchambers were first assembled with laser-cut parafilm gaskets sandwiched by two pieces of glass coverslips as previously described.[18] The volume of microchamber is about 10 µL. Assembled chambers were coated with anti-digoxigenin antibody by incubating with 8 µg/mL anti-digoxigenin (Roche Diagnostics) for 90 minutes at room temperature, then passivated by incubating with Blocking buffer (PBS with 1% caesin, GeneTex) for 20 minutes at room temperature. Transcription tethers were assembled by mixing 30 nM of RNAP holoenzyme and 3 nM linear DNA template in Transcription Buffer (20 mM Tris glutamate pH = 8, 50 mM potassium glutamate, 10 mM magnesium glutamate, 1 mM DTT, 0.2 mg/ml casein) and incubated 20 min at 37°C. Afterwards, 50 µM ATP, UTP, GTP (NewEngland Biolabs), and 100 µM GpA dinucleotides (TriLink) were added to the solution and incubated for additional 10 min at 37°C. After this step, the ternary complex initiated transcription and stalled at the first G in the template. The ternary complex solution was diluted to a final concentration of 250 pM of the RNAP:DNA complex, flushed into the passivated microchamers, and incubated for 10 minutes. Afterwards, 20 µL of streptavidin-coated superparamagnetic beads (diluted 1:100 in Transcription buffer; MyOneT1 Dynabeads, Invitrogen/Life Technologies) were flushed into microchambers and resulted in the attachment of the beads to biotinylated

RNAp stalled on the DNA. Excessive superparamagnetic beads in solution were then cleaned by flushing microchambers with 50 µL Transcription buffer.

Magnetic Tweezers Assays

Magnetic Tweezers were used to observe the dynamics of transcribing TECs by recording the real-time changes in tether length as previous described. The MTs consists of permanent magnets positioned above the microchamber that can be translated along to vary the strength of a laterally oriented magnetic field. The magnitude of tension can be calibrated from the Brownian motion within the x-y plane with the knowledge of tether lengths. Roadblock proteins were diluted to 20 nM for LacI and 45 nM for EcoRI Q111 for optimal binding. The concentrations of LacI proteins were chosen based on previous looping experiments, and the concentration of EcoRI Q111 was selected by identifying the best binding efficiency from AFM images at different concentrations. The diluted roadblock proteins were flushed into microchambers and incubated for 10 minutes at room temperature prior to recording. Excessive roadblock proteins were then flushed out of the chamber with 40 of Transcription buffer to prevent repetitive binding events. After 3 minutes of recording, a full set of NTPs was flushed into chambers to resume transcription of CTP-starved TECs. Recordings lasted at least 30 minutes for weak roadblock systems, and more than one hour for the observation of indefinitely stalled RNAP.

Data Analysis

Prior to data analysis, we inspected the recordings to remove intervals with irregularities. The irregularities may result from buffer injections or temporary tracking failures, and these are evident due to unusual fluctuations. These portions were manually replaced with NaN values and discarded from further analysis. In most traces, this step only discarded data during the introduction of NTPs or GreA. Next, we applied a Bayesian step change detection algorithm to the noisy raw data and extracted step-wise changes in tether lengths. The

method is achieved by minimizing the cost function

$$\text{argmin}_y \left(\sum_i (y_i - \hat{y}_i)^2 + \lambda \sum_i |\hat{y}_{i+1} - \hat{y}_i| \right),$$

where $\hat{y}$ is the smoothed time series and y is raw time series. The method, which is described in detail elsewhere, reliably produced monotonic traces. The smoothed data consists of flat regions separated by sharp jumps, and these are perfectly suitable for detecting paused states in following steps. In theory, positions of transcribing TECs along DNA templates can be calculated from the end-to-end distance of tether with the knowledge of force on the tether and the worm-like chain parameters of the DNA template. However, since there are small uncertainties in the force magnitude from tether to tether due to variation in bead sizes magnetic susceptibilities, each individual trace is linearly rescaled to align the prominent dwell times at promoter, roadblock and terminator positions. FOr this purpose, we converted the smoothed, monotonically increasing or decreasing traces to dwell time histograms. Since the smoothed traces change in a strict step-wise manner, the histograms consist of sharp peaks presenting the duration and position of pause sites. Next, we applied combinations of expansion factor a and a shift factor b to the histograms, generated a new set of histograms $S' = a * S + b$, and found the histogram that presents longest pause durations at the expected positions of promoter, roadblock and terminator. Since the start point of transcription was set to 0 and always presents a significant pause, the shift factor is effectively 0 in this rescaling process. The best-fit values of expansion factor a range from 0.75 to 0.95, depending on the force magnitude in the experiments. Pauses at the roadblock sites in the rescaled histograms were treated as roadblock-induced pauses.

Acknowledgement

LacI was a generous gift from Kathleen Matthews, Rice University. This work was supported by the National Institutes of Health (NIH) grants R01 GM084070 to LF and R01 GM067153

to IA.

References

(1) Ren, B.; Robert, F.; Wyrick, J. J.; Aparicio, O.; Jennings, E. G.; Simon, I.; Zeitlinger, J.; Schreiber, J.; Hannett, N.; Kanin, E.; Volkert, T. L.; Wilson, C. J.; Bell, S. P.; Young, R. A. Genome-Wide Location and Function of DNA Binding Proteins. *Science* **2000**, *290*, 2306–2309.

(2) Kadonaga, J. T. Regulation of RNA Polymerase II Transcription by Sequence-Specific DNA Binding Factors. *Cell* **2004**, *116*, 247–257.

(3) Ramji, D. P.; Foka, P. CCAAT/enhancer-binding proteins: structure, function and regulation. *Biochemical Journal* **2002**, *365*, 561–575.

(4) Wilkins, B. J.; Rall, N. A.; Ostwal, Y.; Kruitwagen, T.; Hiragami-Hamada, K.; Winkler, M.; Barral, Y.; Fischle, W.; Neumann, H. A Cascade of Histone Modifications Induces Chromatin Condensation in Mitosis. *Science* **2014**, *343*, 77–80.

(5) Halford, S. E.; Marko, J. F. How do site-specific DNA-binding proteins find their targets? *Nucleic Acids Research* **2004**, *32*, 3040–3052.

(6) Shen, B. A.; Landick, R. Transcription of Bacterial Chromatin. *Journal of Molecular Biology* **2019**, *431*, 4040–4066, RNA polymerase reaches 60.

(7) Epshtein, V.; Toulmé, F.; Rahmouni, A.; Borukhov, S.; Nudler, E. Transcription through the roadblocks: the role of RNA polymerase cooperation. *The EMBO Journal* **2003**, *22*, 4719–4727.

(8) Proshkin, S.; Rahmouni, A. R.; Mironov, A.; Nudler, E. Cooperation Between Translating Ribosomes and RNA Polymerase in Transcription Elongation. *Science* **2010**, *328*, 504–508.

(9) Lewis, D. E.; Komissarova, N.; Le, P.; Kashlev, M.; Adhya, S. DNA Sequences in gal Operon Override Transcription Elongation Blocks. *Journal of Molecular Biology* **2008**, *382*, 843–858.

(10) Rullens, P. M.; Kind, J. Attach and stretch: Emerging roles for genome–lamina contacts in shaping the 3D genome. *Current Opinion in Cell Biology* **2021**, *70*, 51–57, Cell Nucleus.

(11) Zhou, J.; Ha, K.; La Porta, A.; Landick, R.; Block, S. Applied Force Provides Insight into Transcriptional Pausing and Its Modulation by Transcription Factor NusA. *Molecular Cell* **2011**, *44*, 635–646.

(12) Depken, M.; Galburt, E. A.; Grill, S. W. The Origin of Short Transcriptional Pauses. *Biophysical Journal* **2009**, *96*, 2189–2193.

(13) Qian, J.; Dunlap, D.; Finzi, L. Thermodynamic model of bacterial transcription. *Phys. Rev. E* **2022**, *106*, 044406.

(14) Neuman, K. C.; Abbondanzieri, E. A.; Landick, R.; Gelles, J.; Block, S. M. Ubiquitous Transcriptional Pausing Is Independent of RNA Polymerase Backtracking. *Cell* **2003**, *115*, 437–447.

(15) Svetlov, V.; Artsimovitch, I. Purification of bacterial RNA polymerase: tools and protocols. *Methods Mol Biol* **2015**, *1276*, 13–29.

(16) Perederina, A. A.; Vassylyeva, M. N.; Berezin, I. A.; Svetlov, V.; Artsimovitch, I.; Vassylyev, D. G. Cloning, expression, purification, crystallization and initial crystallographic analysis of transcription elongation factors GreB from *Escherichia coli* and Gfh1 from *Thermus thermophilus*. *Acta Crystallographica Section F* **2006**, *62*, 44–46.

(17) Vassylyeva, M. N.; Svetlov, V.; Dearborn, A. D.; Klyuyev, S.; Artsimovitch, I.; Vassy-

lyev, D. G. The carboxy-terminal coiled-coil of the RNA polymerase β-subunit is the main binding site for Gre factors. *EMBO reports* **2007**, *8*.

(18) Ding, Y.; Manzo, C.; Fulcrand, G.; Leng, F.; Dunlap, D.; Finzi, L. DNA supercoiling: A regulatory signal for the repressor. *Proceedings of the National Academy of Sciences* **2014**, *111*, 15402–15407.